Pattern of Insulin Delivery after Intravenous Glucose Injection in Man and Its Relation to Plasma Glucose Disappearance

ELEUTERIO FERRANNINI and ALESSANDRO PILO, *Consiglio Nazionale delle Ricerche (C.N.R.), Clinical Physiology Laboratory, University of Pisa, 56100 Pisa, Italy*

ABSTRACT Plasma insulin concentrations after pulse intravenous injection of glucose show an early rise, which declines towards the prestimulation level smoothly. This pattern is the effect of both continuing secretion and hormone disappearance from the plasma. To reconstruct the time-course of the actual secretory response, we measured insulin disappearance from the plasma of 17 healthy volunteers by means of a bolus intravenous injection of ^{125}I-insulin, and then performed an intravenous glucose tolerance test with frequent blood sampling. The data were analyzed by deconvolution, which made it possible to compute the glucose-induced posthepatic insulin delivery rate minute by minute.

Under basal conditions, 2.64±0.28 (mean±SEM) mU/min·m^2 reaches the systemic circulation. In the 90 min that follow acute glucose stimulation, 0.86±0.11 U/m^2, a 270% increment over the basal production rate, is made available to the periphery. A wide individual variability was found to exist in both the basal and the glucose-stimulated delivery. They were strongly ($P < 0.001$) related to each other in a direct fashion.

A first spike of insulin release (107±12 mU/min) occurred in all the subjects at 2.2±0.2 min followed, in 16 subjects, by a second spike (38±6 mU/min), at 11.3±0.9 min. Two-thirds of the total postglucose insulin output were associated with the initial, oscillatory phase (from 0 to 25 min, on average), and one-third with the "tail" phase (from 25 to 90 min), during which the average delivery rate was 5.0±0.9 mU/min·m^2.

The delivery curves were closely (mean squared deviation of 4.5±0.5 mU/min) reproduced by computer simulation upon assuming that insulin secretion is a function of both glucose concentration and glucose rate of change.

Both the first and the second spike of insulin delivery, but not the total insulin output during the test, showed a significant, positive correlation with the plasma glucose disappearance rate computed between 10 and 60 min. Furthermore, with a time shift of ≅15 min, a significant relationship between the phases of insulin secretion and the glucose decay rates, computed over corresponding time intervals, was evident throughout the test.

Received for publication 11 April 1978 and in revised form 5 March 1979.

INTRODUCTION

The intravenous administration of glucose is widely used to test the effect of hyperglycemia per se on insulin secretion, and, in turn, the contribution of insulin secretion to glucose tolerance (1). In fact, when glucose is ingested, neural factors and gastrointestinal hormones (2, 3) interfere with the glucose-insulin feedback loop.

Prolonged glucose infusion in man gives rise to a biphasic insulin response (4). This response has been extensively studied both in vivo (5, 6) and in the perfused rat pancreas preparation (7), and hypotheses on the structure of the secretory system of the β-cell have been put forward (5, 6, 8). When glucose is given intravenously as a short injection, a quick rise in plasma insulin concentration is found in the normal subject, presumably representing the discharge of an acutely releasable pool (5). The magnitude of this early response, which is related to the amount of glucose administered (9), is reputed to be an important determinant of glucose tolerance, measured as the plasma glucose disappearance rate (9, 10). After the initial peak, the glucose-stimulated insulin levels fall back to basal with an average half-time of ≅30 min (Fig. 1), much slower than the half-time of plasma insulin (5–10 min). The following questions then arise: (*a*) how much insulin is released after the first peak, and in what time-course, (*b*) what are the signals for

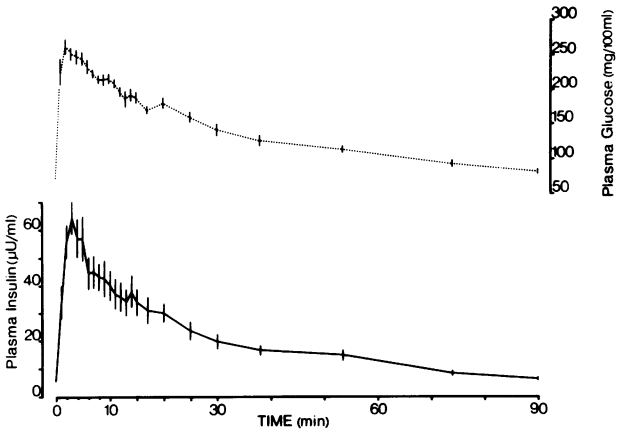

FIGURE 1 Mean plasma insulin (—) and glucose (· · · · ·) concentrations after intravenous injection of 0.33 g of glucose/kg body wt in 17 normal subjects. The vertical bars denote ±SEM.

this continued secretion, and (*c*) what are its effects on glucose disappearance from plasma.

To answer these questions, we used deconvolution analysis (11), by which the postglucose insulin concentration curve, sampled at frequent intervals, and the plasma insulin disappearance curve, measured in the same subject by means of ^{125}I-insulin, are used to compute the insulin delivery rate function minute by minute. In fact, rapid changes in the delivery rate may be smoothed out by the delay introduced by the distribution and clearance of plasma insulin. The features and limitations of this approach have been presented in detail elsewhere (12). In this paper, we report the results obtained in a group of 17 normal subjects, who each received a standard glucose challenge by the intravenous route (intravenous glucose tolerance test [GTT][1] [ivGTT]). The insulin delivery curves thus obtained were analyzed in two ways: as the effect of the glucose stimulus, and as the cause of plasma glucose decline.

METHODS

Study subjects. Subjects were ambulatory, healthy volunteers (Table I). They had negative family histories of diabetes mellitus, and their oral GTT (100 g) was within the normal limits (13). They consumed the average Italian diet (43–48% carbohydrate, 12–17% proteins, and 35–40% fat), and were instructed to maintain normal food intake and activities for 3 d before the study. They were taking no medication and had had no recent change in body weight. All subjects gave informed consent to the study.

Experimental protocol. The studies were performed in the sitting position, at 9 a.m., after an overnight fast. Thyroid uptake had been previously blocked by oral administration of saturated potassium iodide. A plastic cannula was inserted

[1] *Abbreviations used in this paper*: BIDR, basal insulin delivery rate; GTT, glucose tolerance test(s); ivGTT, intravenous GTT; ivGTT-ID, insulin delivered during ivGTT; IRI, immunoreactive insulin; KG, plasma glucose fractional disappearance rate(s); MCR, metabolic clearance rate.

TABLE I
Clinical Characteristics of Subjects

Case	Sex	Age	Height	Weight	Body surface area	Obesity index*
		yr	*cm*	*kg*	m^2	%
1	F	21	165	55	1.6	97
2	F	28	157	56	1.6	104
3	M	26	174	77	1.9	108
4	F	25	150	44	1.4	88
5	F	30	162	59	1.6	99
6	F	54	158	43	1.4	69
7	M	36	173	78	1.9	107
8	F	35	168	56	1.6	89
9	F	35	167	58	1.6	93
10	F	16	155	41	1.3	84
11	F	35	157	63	1.6	111
12	F	57	158	48	1.5	77
13	M	32	170	75	1.9	105
14	F	55	147	59	1.5	104
15	F	40	168	63	1.7	94
16	F	27	159	52	1.5	95
17	F	46	159	62	1.6	101
Mean		35	162	58	1.6	96
SEM		3	2	3	0.04	3

* Based on Metropolitan Life Insurance Co. tables.

in an antecubital vein and kept patent by intermittent flushing with isotonic saline. In a typical experiment, after a stabilization period of 15–20 min, 140–150 μCi of ^{125}I-insulin was injected as a single bolus into a contralateral antecubital vein, and blood samples were collected through the cannula at 2, 2.5, 3, 4, 5, 7, 9, 12, 15, 17, 20, 25, and 30 min, and then every 10 min until 2 h. After another 20 min, 0.33 g/kg of body weight glucose (as a 40% aqueous solution) was rapidly (usually 2 min) infused into a peripheral vein, and blood samples were obtained every min for 15 min, and then at 17, 20, 25, 30, 35, 40, 50, 60, 75, and 90 min for glucose and insulin determination. Zero time was taken to be the mid-injection time, and, therefore, is actually 1 min after the start of glucose injection. Blood was drawn into tubes which contained EDTA; plasma was promptly separated by centrifugation, and stored at −20°C until assayed.

Tracer. [^{125}I]Monoiodoinsulin was prepared by the lactoperoxidase method (14), as modified by Citti et al. (15). Purification and characterization of the tracer was performed as previously described (16). Subjects 1–6 received a tracer having an 8–10 mCi/mg sp act; in the remaining subjects, a tracer with much higher (100–200 mCi/mg) specific activity was used for injection. The two mixtures showed identical kinetics (16). In all cases, the tracer was used within 24 h of preparation.

Analytical procedures. Immunoprecipitable radioactivity was measured in triplicate by a modification (16) of the double antibody immunoprecipitation technique of Hales and Randle (17). Plasma concentration of endogenous insulin (immunoreactive insulin [IRI]) was measured as described (18), or with ^{131}I-insulin as labeled antigen. Separation of bound from free insulin was accomplished with the use of dextran (Pharmacia Fine Chemicals, Div. Pharmacia, Inc., Piscataway, N. J.) -coated charcoal and centrifugation at 3,000 *g*. The inter- and intra-assay variation coefficients were 14 and 7%, respectively (19), in the range of basal concentrations (3–20 μU/ml). Samples were diluted so that most readings fell into the above range.

Plasma glucose concentration was measured in duplicate by the glucose oxidase method (20) on a Beckman Analyzer (Beckman Instruments, Inc., Fullerton, Calif.). The error in this assay was <3%.

Data analysis

Insulin delivery, $\bar{D}(t)$, is related to insulin concentration, $\bar{I}(t)$, and plasma ^{125}I-insulin disappearance, $P(t)$, normalized by the injected dose, according to the following equation:

$$\bar{I}(t) = \bar{D}(t) * P(t)/\text{dose} \quad (1)$$

where * indicates the convolution product. We experimentally determined the impulse response of the insulin system, $P(t)$/dose, by a single injection of ^{125}I-insulin, and measured the insulin concentration after the glucose load, $\bar{I}(t)$; therefore, Eq. 1 can be solved for $\bar{D}(t)$. The minute by minute computation of $\bar{D}(t)$ from the integral Eq. 1, known as deconvolution analysis, was accomplished by means of an iterative numerical method, reported elsewhere (12). Because deconvolution generates oscillating solutions, the computation method included a smoothing process, which had been adjusted to the experimental within-assay error in plasma insulin measurement (≅7%) (Analytical procedures). This criterion proved practical, because computed delivery functions are relative insensitive even to largely misjudged assay errors. The formulas used to calculate the insulin parameters are listed below:

$$\text{MCR} = \text{Dose} \Big/ \int_0^\infty P(t)dt \quad (2)$$

$$\text{BIDR} = \text{MCR} \cdot \text{fasting IRI} \quad (3)$$

$$\text{ivGTT-ID} = \int_0^{90} \bar{D}(t)dt \quad (4)$$

$$\text{Mean time} = \frac{\int_0^{90} t\bar{D}(t)dt}{\int_0^{90} \bar{D}(t)dt} \quad (5)$$

where MCR is the metabolic clearance rate, BIDR is the basal insulin delivery rate to the systemic circulation, and ivGTT-ID is the total amount of insulin delivered during the ivGTT.

If it is assumed that both $\bar{D}(t)$ and $\bar{I}(t)$ return to their respective base-line level by the end of the experimental period (90 min), integration of Eq. 1 will give the following equation:

$$\text{ivGTT-ID} = \text{MCR} \int_0^{90} \bar{I}(t)dt \quad (6)$$

in which the total amount of insulin delivered in 90 min can also be estimated from the insulin area-under-curve (inclusive of the basal insulin level), and the MCR.

The main oscillations in the insulin delivery rate curves were identified as follows: a peak of insulin secretion was considered to have occurred when the delivery rate rose in two or more successive time intervals, and the difference between the peak value and the preceding minimum was at least 4 mU/min. This threshold is arbitrary; it corresponds, for a MCR value of 800 ml/min, i.e., the normal average value (16, 21), to a difference in plasma insulin concentration of 5 μU/ml. This is equivalent to assuming that the plasma insulin was measured with an error of 5 μU/ml, which is 25% of the mean postglucose insulin concentration found in our subjects, and is more than three times greater than the experimental within-assay relative insulin error (7%). This criterion is restrictive, if compared, for example, with the widely adopted (22) criterion that uses the cumulative standard deviation of the measurements as the threshold. However, this restriction was felt to be suitable, because the oscillations in insulin delivery usually occur early (within 25 min of glucose injection), when insulin levels are still high.

Simulation of the insulin delivery functions was performed by assuming that the insulin delivery rate depends upon plasma glucose through both a derivative and a (so-called) proportional action. These actions are each weighted for the coefficients CD and CP, respectively, according to the following equation:

$$\bar{D}_s(t) = \text{CD} \cdot G'(t) * k_1 e^{-k_1 t} + \text{CP} \cdot G_{hm}(1 + \tanh S[G(t) * k_2 e^{-k_2 t} - G_{hm}]) \quad (7)$$

where $G(t)$ is the plasma glucose concentration, $G'(t)$ is its derivative, k_1 = 0.693/half-time 1, and k_2 = 0.693/half-time 2 are the slopes of the time lags applied to $G'(t)$ and $G(t)$, respectively, and G_{hm} and S are the half-maximum and the slope, respectively, of the sigmoidal function linking insulin delivery with plasma glucose concentration. Equal (1 min) spacing of the experimental values for plasma glucose con-

centration was obtained by interpolation. $\bar{D}_s(t)$ was fitted on $\bar{D}(t)$, minute by minute, using the least squares method. The values of CD and CP, in which Eq. 7 is linear, were derived from normal equations. The optimizing values for G_{hm}, S, k_1, and k_2 were obtained by exhaustive search within sets of four values for each of these parameters in the following ranges: 110–170 mg/100 ml for G_{hm}; 0.005–0.06 for S; 0.17–1.4%/min for k_1, and 0.3–1.5%/min for k_2. These ranges were themselves established by a trial and error method.

Plasma glucose fractional disappearance rates (KG) were computed by linear regression analysis of the natural logarithms of plasma glucose concentration, over the indicated time interval. Glucose mean time was calculated in the same way as the mean time of insulin delivery (Eq. 5). Glucose and insulin area-under-curve were computed by trapezoidal integration of the respective incremental values over the fasting level.

All calculations were done with the aid of a digital computer.

RESULTS

Insulin delivery curve. The mean insulin concentration curve is shown in Fig. 1; the individual values of the insulin area-under-curve are given in Table II. Fig. 2 shows the average plasma disappearance curve of ^{125}I-insulin. The mean and the scatter of the MCR values calculated from the individual ^{125}I-insulin decay curves (Table II) are virtually superimposable on the values (451±18 ml/min·m^2) obtained by Sherwin et al. (21) in 16 normal subjects with the use of unlabeled insulin. The BIDR, derived as the product of MCR by the fasting IRI level (Table II), showed a wide dispersion (coefficient of variation = 45%), indicating that normal subjects in the postabsorptive state need very different amounts of insulin to maintain similar glycemic levels (fasting plasma glucose was 77±10 mg/100 ml, mean±SD). Likewise, the ivGTT-ID showed a high degree of individual variability (coefficient of variation ≅50%).

Fig. 3 shows a typical insulin delivery rate curve, computed from the insulin concentration and the plasma ^{125}I-insulin disappearance curve by means of deconvolution. An oscillatory pattern, with two or three spikes of insulin secretion, occurred in the first 25 min after the acute glucose stimulation; this pattern was followed by a phase during which insulin release returned smoothly towards the basal levels. It was noteworthy that this pattern was maintained despite the fact that the total amount of hormone secreted by our study subjects in response to the glucose stimulus varied over a six- to sevenfold range. Table III summarizes the results of the resolution of the individual insulin delivery rate curves, performed according to the criteria defined in Methods. A first peak of insulin delivery, occurring 2.2±0.2 min after glucose injection, and lasting 7±0.6 min, was found in all the subjects. Because zero time was taken to be about 1 min on average after the start of glucose injection, the first peak time was actually 3.2 min. By taking into account the delay introduced by the circulation times (vis-à-vis glucose to pancreas, and insulin to posthepatic veins [23]) it can be estimated that the maximal response of the β-cell to glucose occurs in <1 min, in accord with

TABLE II
Insulin Parameters

Case	MCR	Fasting IRI	BIDR	Insulin area	ivGTT-ID	Mean time
	ml/min·m²	*μU/ml*	*mU/min·m²*	*mU/ml·min*	*mU/m²*	*min*
1	314	5.0	1.57	1.23	547	6.1
2	404	5.3	2.15	0.96	604	23.8
3	300	5.2	1.57	1.59	656	27.4
4	299	8.0	2.40	1.77	756	13.5
5	551	4.4	2.43	0.69	627	22.4
6	515	3.2	1.65	0.21	246	31.3
7	511	4.8	2.45	1.54	1060	13.5
8	549	6.9	3.78	1.77	1390	18.7
9	568	6.0	3.42	0.78	797	27.9
10	514	5.0	2.57	0.83	683	30.0
11	448	3.3	1.48	1.57	877	27.5
12	407	4.3	1.75	0.60	419	30.2
13	544	6.7	3.65	2.57	1840	28.1
14	460	7.2	3.32	1.04	841	35.0
15	390	3.2	1.25	0.50	317	14.6
16	538	10.2	5.48	2.30	1770	31.5
17	433	9.1	3.93	1.88	1240	24.3
Mean	456	5.8	2.64	1.28	862	23.9
SEM	22	0.5	0.28	0.16	112	1.9

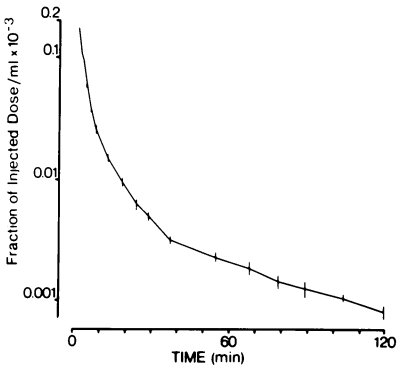

FIGURE 2 Logarithmic plot of the mean plasma disappearance curve of ^{125}I-insulin after pulse intravenous injection of 140–150 μCi of tracer in 17 normal subjects. The vertical bars denote ±SEM.

direct estimates (24). 16 subjects (91%) also showed a second peak, which appeared 11.3±0.9 min after glucose injection, and lasted 14±1 min. This second burst of insulin delivery was characterized by a maximal rate about two and one-half times lower than the first peak; however, because its duration was twice as long, the total insulin output during this phase was similar to that associated with the first peak. In seven subjects (41%), a third, smaller oscillation was recognizable 19.9±1.8 min after glucose administration. A smooth phase, or "tail," of insulin response was generally detected during the last 65±2 min of the test. The mean delivery rate curve, obtained by averaging all the values at 1-min intervals, is shown in Fig. 4. In this plot, a "phasic" pattern is still recognizable, even though the time averaging has obviously smoothed out the individual oscillations that were not in-phase.

TABLE III
Characteristics of the Insulin Delivery Rate Curve after Intravenous Glucose

	Mean*	SEM	Range
First peak			
Duration, *min*	7	0.6	4–13
Maximum rate, *mU/min*	107	12	43–181
Output, *mU/m²*	270	34	94–565
Fraction of total output, %	33	3	18–56
Second peak			
Duration, *min*	14	1	7–27
Maximum rate, *mU/min*	38	6	7–83
Output, *mU/m²*	223	33	23–469
Fraction of total output, %	25	3	9–57
Third peak			
Duration, *min*	12	2	6–22
Maximum rate, *mU/min*	31	5	14–60
Output, *mU/m²*	141	22	42–304
Fraction of total output, %	15	3	7–22
Tail			
Duration, *min*	65	2	47–82
Output, *mU/m²*	327	64	0–913
Fraction of total output, %	36	4	0–56

* According to the criteria defined in the Methods, a first peak was recognizable in 17, a second peak in 16, and a third peak in 7 of 17 subjects. Because the mean values for the fractional insulin outputs refer to different number of subjects, their sum is not 100%.

The mean time, or center of gravity, of the insulin delivery functions, which is an index of the relative time distribution of insulin output, was found to be 24 min on average (Table II), ranging from as little as 6 min to over 30 min. Indeed, about two-thirds of the insulin released was concentrated in the first 25 min after the glucose challenge, regardless of the total

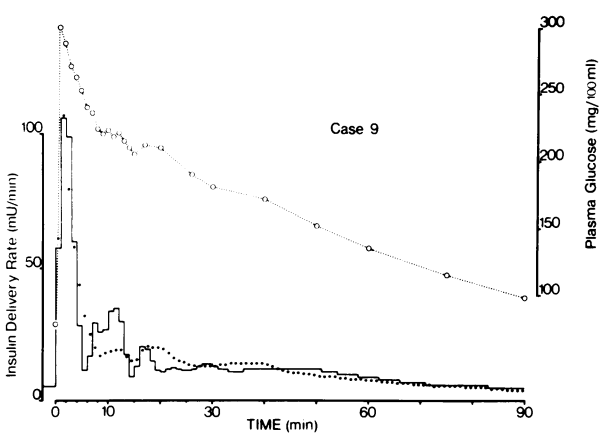

FIGURE 3 The minute by minute delivery rate of insulin into the systemic circulation after intravenous glucose is shown here by the full line. The open circles indicate the experimental plasma glucose concentrations. The closed circles are the values of the computer-matched insulin delivery rate $\bar{D}_s(t)$, derived from the plasma glucose concentration $G(t)$ according to the following equation (Data Analysis): $\bar{D}_s(t) = 6.0 \cdot G'(t) * 0.35e^{-0.35t} + 0.26 \cdot 110(1 + \tanh 0.03[G(t) * 0.6e^{-0.6t} - 110])$. Data is from subject 9.

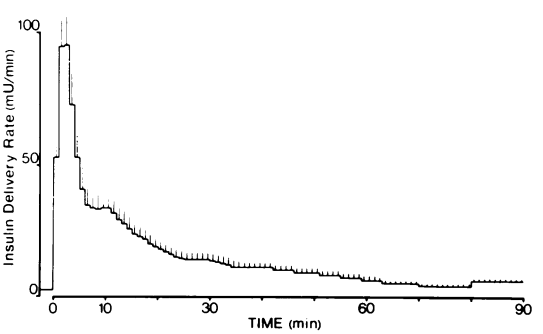

FIGURE 4 Mean posthepatic insulin delivery rate after intravenous glucose injection in 17 normal subjects. The vertical bars indicate 1 SEM.

amount of insulin produced during the whole test. Correspondingly, no correlation was found to exist between ivGTT-ID and the mean time of the insulin delivery curves. In contrast, the basal delivery rate and the overall glucose-induced insulin production were found to be highly significantly associated in a positive manner (Fig. 5).

Glucose curve. The mean plasma glucose concentrations at the sample times are reported in Fig. 1. In some subjects, the decline in plasma glucose during the first 15–20 min was markedly irregular (e.g., Fig. 3). This behavior is also visible in the mean curve (Fig. 1). The 3- to 5-min increment in plasma glucose over the fasting level was 175 mg/100 ml on average, with a variation coefficient of ≅20%, which suggests that the initial distribution volume of the injected glucose did not vary much in this group of subjects. When plotted in semilogarithmic scale, the time-course of plasma glucose concentration was not monoexponential. In a first approximation, a faster slope followed the initial peak value for about 25 min; the glucose then declined at a slower rate. The KG values computed between 3 and 25 min after injection (2.21±0.16%/min) were thus significantly ($P < 0.01$) higher than those computed between 25 and 90 min (1.00±0.07%/min). The KG commonly used in the evaluation of the ivGTT, i.e., those computed between 10 and 30 min (9), and between 10 and 60 min (2), differed significantly ($P < 0.05$) from each other (Table IV). Generally, it was found that the greater the distance between the starting point of interpolation and the injection time, the lower the KG value (e.g., KG_{10-40} = 1.86±0.19, KG_{20-50} = 1.67±0.22, KG_{30-70} = 1.11±0.07, and KG_{40-90} = 0.87±0.11%/min). Furthermore, the glucose area-under-curve (Table IV), as well as the glucose mean time, which are integral indexes of the glucose curve, were both found to be best correlated ($r \geq -0.76$, $P < 0.001$) with the KG computed from 10 to 40–60 min. This means that those curves which fall more steeply during this time interval are associated with lower overall increments of plasma glucose over the fasting level during the test. In addition, the glucose decay rate between 40 and 90 min was inversely correlated ($r = 0.60$, $P < 0.01$) with the glucose area. This consistently indicates that those curves which had fallen to lower concentrations within about 40 min of injection showed a slower decline thereafter, whereas, if plasma glucose were still relatively high at that time (greater glucose area), then the following decrease rate was relatively accelerated.

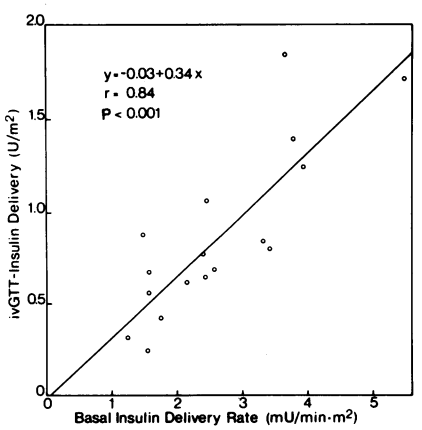

FIGURE 5 Relationship between basal systemic insulin delivery rate and glucose-induced insulin delivery in 17 normal subjects.

An interesting finding was that the fasting glucose level and the glucose disappearance rate from 3 to 25 min after injection were significantly correlated ($r = 0.59$, $P < 0.05$) in a reciprocal manner.

Relationship between plasma glucose and insulin delivery. Simulation of ivGTT-ID was attempted with an equation (Data analysis) in which the insulin delivery rate is a function both of glucose concentration and of glucose rate of change. To fit the data satisfactorily, this simple dependence had to be modified in the following way. First, it was assumed that insulin secretion is related to plasma glucose concentration (proportional action) according to a sigmoidal function (Fig. 6). Second, both the derivative and the proportional control were lagged by a suitable time to account for the fact that insulin secretion responds to glucose with some delay, and that arterial plasma glucose is reflected with a time shift on the venous side of the circulation.

Fig. 7 shows an example of this simulation. It can be seen that the derivative control is quantitatively predominant in the first 10 min after injection, whereafter it becomes mostly negative, thus bringing about an inhibitory effect. Such rate-sensitive control also accounts for the secondary oscillations in insulin secretion observed between 6 and 25 min, because during this time interval plasma glucose often shows fast changes in slope. This phenomenon has been observed when continuously monitoring plasma glucose during ivGTT (25). The proportional action, in contrast, takes the form of a plateau, which declines slowly and regularly, and accounts for most of the secretion occurring from 10 min until the end of the experiment, when the contribution of the derivative action tends to be nil.

Table V summarizes the results of the simulation in our group of subjects. The lags of the two actions were comparable, and the coefficient for the derivative term was, on average, 15 times greater than that of the proportional term. In Fig. 6, the relationship between insulin release and plasma glucose concentration was

TABLE IV
Glucose Parameters

Case	FPG*	Δ3-5 MG‡	GA_{0-90}§	KG_{10-30}	KG_{10-60}	Mean time
	mg/100 ml	*mg/100 ml*	*g/100 ml·min*	*%/min*	*%/min*	*min*
1	73	142	2.59	4.42	3.10	10.8
2	91	178	8.23	1.14	1.14	34.5
3	94	177	6.12	1.78	1.33	27.3
4	70	185	4.46	2.45	1.83	19.4
5	60	173	4.01	2.26	1.64	22.4
6	75	146	5.78	1.50	1.08	30.7
7	79	122	2.43	2.94	2.30	13.6
8	76	113	3.31	1.81	1.49	21.7
9	78	184	7.79	0.95	1.00	31.7
10	67	154	6.24	1.37	1.01	32.7
11	80	181	5.26	1.75	1.40	25.1
12	72	194	6.70	1.83	1.45	28.8
13	70	174	4.69	2.02	1.85	20.4
14	88	193	6.35	1.70	1.38	25.7
15	64	199	6.15	2.09	1.29	28.9
16	84	263	7.11	1.97	1.61	24.8
17	89	205	6.14	2.03	1.59	23.5
Mean	77	175	5.49	2.00	1.56	24.8
SEM	2	8	0.41	0.19	0.13	1.6

* Fasting plasma glucose concentration.
‡ 3–5 min mean glucose increment over the fasting level.
§ Glucose area from 0 to 90 min.

drawn with the mean group values for the parameters, given in Table V. It can be seen that, in this ideal average case, the insulin response to hyperglycemia is linear between 100 and 200 mg/100 ml, and practically saturated for concentrations >300 mg/100 ml. In the range of the low glucose concentrations (60–100 mg/100 ml), the insulin secretory system is relatively less sensitive. In addition, on the same graph, the mean fasting glucose level of our subjects (77 mg/100 ml) corresponds to an insulin delivery rate of 2.7 mU/min, a value comparable to the experimentally observed mean value for BIDR (4.2 mU/min, Table II).

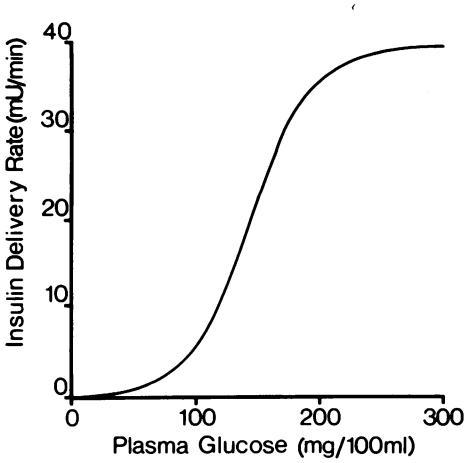

FIGURE 6 Dependence of the insulin delivery rate upon plasma glucose concentration (proportional control). The equation of this sigmoidal function is (Data analysis): Insulin delivery rate = $CP \cdot G_{hm}(1 + \tanh S[G(t) - G_{hm}])$. The function drawn here was obtained with the mean population values for CP, G_{hm}, and S given in Table V. It can be seen that the function tends asymptotically to $CP \cdot G_{hm} \cdot 2 = 40.0$ mU/min, and that its maximal derivative is $CP \cdot G_{hm} \cdot S = 0.4$ mU·100 ml/min·mg, when $G(t)$ is equal to G_{hm}.

Relationship between insulin delivery and plasma glucose disappearance. The relation of insulin response in its various phases to plasma glucose disappearance was examined by correlation analysis. The results are schematized in Table VI. Both of the two main spikes of insulin delivery were found to be significantly correlated with the KG computed between 10 and 60 min, and with the glucose area. This dependence was true of the maximal ($r = 0.49$, $P < 0.05$, and $r = 0.60$, $P < 0.05$, for the first and the second peak, respectively) as well as the average delivery rate (Table VI). In contrast, the KG calculated between 40 and 90 min was directly correlated with the tail phase, and inversely correlated with the two initial peaks of insulin delivery.

When insulin response was evaluated as the average plasma insulin concentration during the time intervals (0–7, 7–25, and 25–90 min) corresponding to the

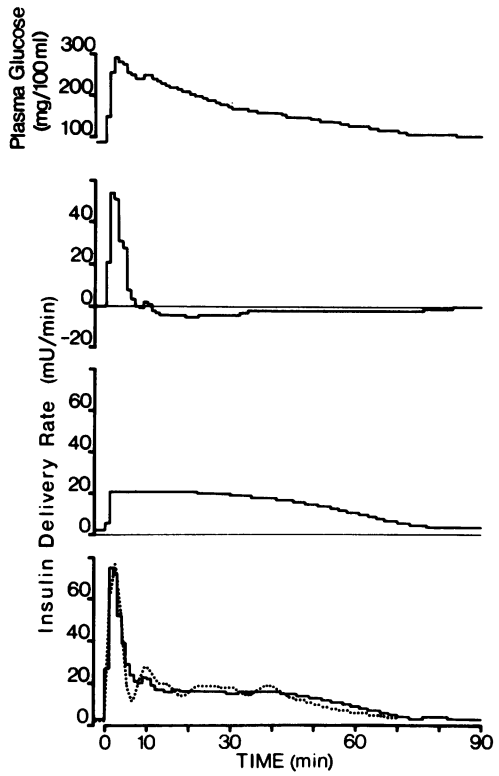

FIGURE 7 Upper panel: plasma glucose concentrations, interpolated at 1-min intervals. Lower panel: experimental (·····) and computer-matched (——) insulin delivery curve. The latter is obtained as the sum of the two curves in the middle panels. These represent the insulin secretion induced by the derivative (upper middle) and the proportional (lower middle) action. The derivative control is the numerical derivative of plasma glucose concentration, lagged by a half-time of 2 min, and multiplied by a weighting coefficient equal to 1.26. The proportional control is the hyperbolic tangent transform of plasma glucose concentration, lagged by a half-time of 0.4 min, and multiplied by 0.08. Data is from subject 3.

mean duration of the three delivery phases, the same pattern of correlations was found. When the delivery (or the plasma insulin) values were normalized by the basal delivery rate (or the fasting plasma insulin, respectively) (26), the dependence of the KG computed between 10 and 60 min upon the early spikes of insulin delivery became stronger (Table VI). However analyzed, the data failed to show a correlation between the initial glucose slope (KG_{3-15}) and insulin delivery. In a like manner, none of the glucose parameters correlated with the ivGTT-ID.

DISCUSSION

When a bolus of tracer insulin is injected into a peripheral vein, its disappearance from the plasma, sampled in another vein, will closely match the disappearance of the endogenous insulin streaming into the systemic circulation through the hepatic veins. In fact, because the two anatomical entry sites are roughly equidistant from the right atrium, the principal requisite of the tracer method, that the tracer and the tracee enter the system at the same site, is fulfilled. Therefore, a frequently sampled plasma insulin concentration curve can be deconvolved by the tracer disappearance curve to yield the posthepatic delivery rate of the hormone. The posthepatic delivery, in turn, can be used to estimate pancreatic secretion if account is taken of the interposition of the liver. In this regard, there is ample evidence to show that the liver removes approximately one-half of the pancreatic insulin at each transhepatic passage (27) and delays the hormone transit only minimally (28). However, it is still controversial whether insulin extraction by the liver remains constant at insulin levels close to the upper bound of the physiological range (29–31). Thus, from the computed posthepatic delivery curves, insulin secretion can be estimated by applying a scale factor, equal to the reciprocal of hepatic extraction, on the assumption that liver extraction is constant. If, on the other hand, liver extraction changes, some inaccuracies in the estimates are expected at high delivery rates.

With these reservations, this study could establish that, on average, an adult, healthy person of median body build secretes about 13 U of insulin/d under basal conditions (i.e., if the postabsorptive state were maintained for 24 h [32]), and disposes of 20 g of glucose injected intravenously by means of 3 U of insulin in 90 min, a 270% increment over the basal production rate. Normal subjects are likely to be distributed

TABLE V
Parameters of the Simulated Insulin Delivery Rate Functions

	Mean	SEM	Range
Half-time 1*, *min*	1.9	0.3	0.5–4.0
Half-time 2‡, *min*	1.0	0.1	0.4–2.3
Glucose half-maximum§, *mg/100 ml*	143	5	110–170
Slope‖	0.02	0.003	0.01–0.03
CD¶, *mU·100 ml/mg*	2.00	0.44	0.46–6.65
CP**, *mU·100 ml/mg·min*	0.14	0.02	0.03–0.34
CD:CP ratio, *min*	15.4	1.8	3.5–29.3
Square root of the mean squared deviations, *mU/min*	4.5	0.5	1.5–8.7

* Half-time of the lag of the derivative action.
‡ Half-time of the lag of the proportional action.
§ Half-maximum of the sigmoidal function relating insulin delivery rate to plasma glucose concentration.
‖ Slope of the sigmoidal function relating insulin delivery rate to plasma glucose concentration.
¶ Coefficient for the derivative action.
** Coefficient for the proportional action.

TABLE VI

*Relationship between Insulin Delivery Rates and Glucose Disappearance Rates**

	First peak		Second peak		Tail	
KG_{3-15}	0.03	0.12	−0.02	−0.06	0.11	−0.09
KG_{10-30}	0.45	0.77‡	0.36	0.73‡	−0.32	−0.47
KG_{10-60}	0.56§	0.74‡	0.52§	0.80‡	−0.17	−0.37
KG_{40-90}	−0.28	−0.67‡	−0.05	−0.50§	0.64‡	0.68‡
GA_{0-90}	−0.62‡	−0.71‡	−0.47	−0.67‡	0.30	0.33

* The numbers in this Table are the correlation coefficients of the glucose KG, computed over the time intervals indicated in the subscripts, with the average delivery rate during the three main phases of insulin secretion. For each phase, two coefficients are indicated: one (left) refers to the absolute value of the average delivery rate, the other (right) refers to the average delivery rate normalized by the basal delivery rate.

‡ $P < 0.01$.

§ $P < 0.05$.

around these average values with a wide scatter, which indicates that the sensitivity of glucose metabolism to insulin action may differ between subjects over a several-fold span.

The above estimates can also be derived from the product of the postglucose insulin area by the MCR of insulin, with reasonable certainty (Data analysis and [12]). Therefore, the principal advantage of the deconvolution approach appears to be that of defining the time-course of insulin secretion in a reliable manner. Although the delivery curves were smoothed by a control algorithm based on the estimated error of the insulin concentration curve (12), it is nevertheless possible that some of the smallest pulsations recorded were computation artifacts. Conversely, some high-frequency secretory events could be lost to the smoothing. However, the general pattern of the insulin response to acute glucose stimulation, as is described here, is well defined, and common to the majority of subjects. Furthermore, the amounts of hormone released during the various phases are estimated with even better determinacy, because the integrals of the delivery curve are scarcely affected by the assumed error of the insulin assay (12).

The data presented here demonstrate that, in response to a rapid glucose infusion, insulin secretion quickly rises to a maximum which, in most of the cases, is followed by one or two other distinct secretory pulsations, lasting until about 25 min after injection. A multiphasic response to acute glucose injection has also been suggested from direct measurements in the portal vein of humans (33), even within the short period of observation (15 min) employed. The amount of hormone outpoured during the phase (2–25 min on average) in which such secretory spikes occur, makes up for over two-thirds of the ivGTT-ID. In the subsequent period (25–90 min), insulin release usually returns smoothly to the prestimulation rate. A built-in feature of the glucose-induced insulin response is that higher basal production rates are associated with higher glucose-stimulated rates (Fig. 5). The relative time distribution of insulin, as reflected in the mean time of the delivery curve, is independent of the "set point" of the secretory machinery, which, as previously noted, appears to be established by the individual sensitivity to insulin action.

In considering the causes of the observed, multiphasic pattern of hormone discharge, we thought it would be pertinent to attempt to relate insulin release to plasma glucose, as neural or gut factors (2) or counterregulatory hormones (34) are normally not involved in the ivGTT. We found that, assuming insulin secretion depends upon glucose concentration as well as on glucose rate of change (35, 36), the delivery pattern during ivGTT in the normal subject could be simulated with very good approximation (within 4.5 mU/min on average). The inclusion of a rate-sensitive element was needed to reproduce the multiphasic characteristic of the insulin response, and a nonlinear (sigmoidal) dependence of secretion upon glucose level gave a much better fit than a linear control. It should be observed that a nonlinearity can also be incorporated into the derivative element. This nonlinearity, which has been suggested by recent experimental work (35), would avoid the negative values for insulin secretion that are generated when glucose falls very quickly. The resulting relationship would then be the same as that used to govern insulin infusion with the artificial endocrine pancreas (37, 38). However, because in our observations in no case did we obtain negative values for insulin release, we adopted a simpler equation, with fewer parameters to be adjusted. Of note is that the mean ratio of the derivative to the proportional part, found in our subjects,

is in agreement with the in vivo data of Kawamori et al. (39). These investigators performed ivGTT in depancreatized dogs in which insulin was replaced by means of an artificial β-cell with an algorithm similar to ours. They found that the use of ratios between 10 and 20 induced normal glucose curves, minimized the insulin requirement, and prevented hypoglycemia. In these instances, the reported insulin infusion patterns were remarkably similar to the delivery curves of our subjects.

It must be emphasized that the relationship derived in this study is empirical, and does not represent a general model for insulin secretion. In fact, no hypothesis has been made for the structure of the secretory system, which is generally (5, 7, 40), if not unamimously (6), believed to be compartmentalized and sensitive to stimulation with a threshold distribution (7). Consequently, this relationship cannot predict the response to different formats of stimulation (prolonged glucose infusion, sequential pulses, etc.) because known phenomena such as potentiation (41), and attenuation of rate sensitivity (35, 40), are not featured. In all likelihood, these latter processes cannot be reliably identified if only the response to a single rapid glucose stimulus (ivGTT) is analyzed (42). Nevertheless, the observed coupling of insulin delivery to glucose behavior, even when using a simplified relationship, confirms the physiologic nature of the pattern of insulin response to pulse glucose injection, as defined in these studies.

With regard to the effect of glucose-induced insulin release on the disappearance of injected glucose from plasma, a direct relationship between the early insulin response and glucose decay rate has been repeatedly reported (9–11, 36). Reaven and Olefsky (43), on the contrary, did not confirm this observation, as they only found a significant correlation between KG and the plasma insulin value at 10 min. This controversy is probably fueled by differences in the experimental protocol (dose and mode of glucose administration, sampling times, etc.) as well as in the analysis of the results (time interval over which the KG is computed, evaluation of the acute insulin response, etc.). Therefore, we sought correlation between two indices of plasma glucose behavior (the KG and the glucose area) and various estimates of the insulin response (maximal rate, average rate, and average concentration). Several time intervals were used for the calculation of KG, whereas the timing of insulin release was judged both by individual peak analysis and by splitting the response into fixed intervals (0–7, 7–18, and 18–90 min). By all the methods, the KG_{10-60} and the glucose area, which is its best correlate, were found to be significantly influenced by both of the two main pulses of insulin output that occur during the first 25 min of the test.[2] These correlations were modest. However, it could be surmised that differences in the individual sensitivity to insulin would obscure the relationship between insulin output and glucose assimilation. We therefore attempted to reduce the variability of the insulin response by normalizing the insulin outputs by the basal secretion. The rationale for this manipulation is that the stimulated response (ivGTT-ID) is strongly related to the BIDR, which suggests that, in the same person, insulin sensitivity is the same in the fasting and in the stimulated condition. Upon applying this correction, the dependence of glucose disappearance upon acute insulin response was generally strengthened, without changes in the pattern of the correlations (Table VI). Thus, it seems possible to conclude that the insulin secretion occurring early (within 25 min) after the stimulus, in the form of discrete bursts, determines (by ≅60%) the disposal of an intravenous glucose load. This action, presumably exerted through changes in insulin concentration, does not usually become evident before 15–20 min after stimulation, because the plasma glucose decay rate at early times (3–15 min) is independent of the ongoing insulin release. This time shift is likely to reflect the delay in insulin action, in accordance with direct estimates (44).

Our analysis also indicates that glucose disappearance does not correlate with the total insulin output during the test. This finding has been reported by others (43). An explanation can be inferred from the following results: (*a*) the early (10–30 min) and the late (40–90) KG are inversely related to each other; and (*b*) the KG_{40-90} is positively correlated with the fractional output of the tail phase, but inversely related to those of the two peaks. Thus, it can be thought that, if plasma glucose is still relatively high by 25 min, continued stimulation of insulin release is prompted, which results in a surplus of hormone having only little additional effect on the glucose disposal rate between 10 and 60 min. This late secretion, at any rate, will eventually influence glucose clearance from plasma at corresponding times. The rapid insulin discharge can thus be viewed as the attempt to overcome brisk hyperglycemia by means of a "primed" response (45), analogous with what has been described with the artificial pancreas (46, 47). When this prompt delivery succeeds in bringing plasma glucose back to normal, secretion also returns to prestimulation levels (or below); otherwise, both the glucose and the insulin curve will be prolonged.

[2] Estimating the acute insulin response as in (9) (mean incremental insulin between 3 and 5 min) or as in (43) (sum of the absolute insulin concentrations at 1, 3, and 5 min) did not change the result.

This coupling is reflected in the strong, positive correlation that was found to exist between the mean times of the two curves.

It should be borne in mind that this description, though consistent, is largely based on correlations, and bears on the special situation in which an acute glucose load is given by vein. Furthermore, the problem remains of explaining the behavior of plasma glucose concentration during the 10–15 min that follow glucose injection. If it is presumed that, during this time, glucose-induced insulin secretion has not yet displayed its full action, then conceivable factors affecting glucose levels are: mixing and distribution of the injected load, renal spill-over, endogenous glucose production, glucose uptake by insulin-independent tissues, and glucose uptake mediated by basal insulin secretion. Our data provide no information as to how these disparate processes contribute to the irregular glucose profile frequently seen in normal subjects. The observed reciprocal relationship between this early glucose slope and fasting plasma glucose, which is a tightly controlled variable (48), lends itself to some conjecture on the role of glucose clearance in regulating basal plasma glucose level.

ACKNOWLEDGMENTS

The excellent technical assistance of Paolo Cecchetti and Antonio Masoni is very gratefully acknowledged. We are indebted to Dr. Lorenzo Citti for kindly providing the tracer. Mr. Luca Battini was of invaluable help in performing the insulin radioimmunoassay. We should like to thank Mrs. Carol Ann Hacon for revising the manuscript.

REFERENCES

1. Lundbaek, K. 1962. Intravenous glucose tolerance as a tool in definition and diagnosis of diabetes mellitus. *Br. Med. J.* **1:** 1507–1513.
2. Porte, D., Jr., and J. D. Bagdade. 1970. Human insulin secretion: an integrated approach. *Annu. Rev. Med.* **21:** 219–240.
3. DeFronzo, R. A., E. Ferrannini, R. Hendler, J. Wahren, and P. Felig. 1978. Influence of hyperinsulinemia, hyperglycemia and the route of glucose administration on splanchnic glucose exchange. *Proc. Natl. Acad. Sci. U. S. A.* **75:** 5173–5177.
4. Cerasi, E., and R. Luft. 1963. Plasma insulin response to sustained hyperglycemia induced by glucose infusion in human subjects. *Lancet.* **II:** 1359–1363.
5. Porte, D., Jr., and A. A. Pupo. 1969. Insulin response to glucose: evidence for a two pool system in man. *J. Clin. Invest.* **48:** 2309–2319.
6. Cerasi, E., G. Fick, and M. Rudemo. 1974. A mathematical model for the glucose-induced insulin release in man. *Eur. J. Clin. Invest.* **4:** 267–278.
7. Curry, D. L., L. L. Bennett, and G. M. Grodsky. 1968. Dynamics of insulin secretion by the perfused rat pancreas. *Endocrinology.* **83:** 572–584.
8. Grodsky, G. M. 1972. A threshold distribution hypothesis for packet storage of insulin and its mathematical modeling. *J. Clin. Invest.* **51:** 2047–2059.
9. Lerner, R. L., and D. Porte, Jr. 1971. Relationships between intravenous glucose loads, insulin responses and glucose disappearance rate. *J. Clin. Endocrinol. Metab.* **33:** 409–417.
10. Thorell, J. I., B. Nosslin, and G. Sterky. 1973. Estimation of the early insulin response to intravenous glucose injection in man. *J. Lab. Clin. Med.* **82:** 101–110.
11. Turner, R. C., J. A. Grayburn, G. B. Newman, and J. D. N. Nabarro. 1971. Measurement of the insulin delivery rate in man. *J. Clin. Endocrinol. Metab.* **33:** 279–286.
12. Pilo, A., E. Ferrannini, and R. Navalesi. 1977. Measurement of glucose-induced insulin delivery rate in man by deconvolution analysis. *Am. J. Physiol.* **233:** E500–E508.
13. Fajans, D. S., and J. S. Conn. 1959. The early recognition of diabetes mellitus. *Ann. N. Y. Acad. Sci.* **82:** 208–218.
14. Sodoyez, J. C., F. Sodoyez-Goffaux, N. M. Goff, A. E. Zimmerman, and E. R. Arquilla. 1975. ^{127}I- or carrier-free ^{125}I-monoiodoinsulin. Preparation, physical, immunological, and biological properties, and susceptibility to "insulinase" degradation. *J. Biol. Chem.* **250:** 4268–4277.
15. Citti, L., L. Battini, P. Cecchetti, and R. Navalesi. 1977. Monoiodoinsulin specifically substituted on A_{19} tyrosine: preparation, characterization, and determination of the specific radioactivity. *J. Nucl. Med. All. Sci.* **21:** 152–158.
16. Navalesi, R., A. Pilo, and E. Ferrannini. 1978. Kinetic analysis of plasma insulin disappearance in nonketotic diabetic patients and in normal subjects. A tracer study with ^{125}I-insulin. *J. Clin. Invest.* **61:** 197–208.
17. Hales, C. N., and P. J. Randle. 1963. Immunoassay of insulin with insulin-antibody precipitate. *Biochem. J.* **88:** 137–146.
18. Citti, L., E. Ferrannini, L. Battini, and R. Navalesi. 1976. Radioimmunoassay of labeled and unlabeled insulin mixtures. *J. Nucl. Biol. Med.* **20:** 75–78.
19. Pilo, A., and G. C. Zucchelli. 1975. Automatic treatment of radioimmunoassay data: an experimental validation of the results. *Clin. Chim. Acta.* **64:** 1–9.
20. Robin, M., and A. Saifer. 1965. Determination of glucose in biologic fluids with an automated enzymatic procedure. *Clin. Chem.* **11:** 840–845.
21. Sherwin, R. S., U. J. Kramer, J. D. Tobin, P. A. Insel, J. E. Liljenquist, M. Berman, and R. Andres. 1974. A model of the kinetics of insulin in man. *J. Clin. Invest.* **53:** 1481–1492.
22. Vagnucci, A. H., R. H., McDonald, Jr., A. L. Drash, and A. K. C. Wong. 1974. Intradiem changes of plasma aldosterone, cortisol, corticosterone and growth hormone in sodium restriction. *J. Clin. Endocrinol. Metab.* **38:** 761–776.
23. McGuire, E. A. H., J. H. Helderman, J. D. Tobin, R. Andres, and M. Berman. 1976. Effects of arterial versus venous sampling on analysis of glucose kinetics in man. *Am. J. Physiol.* **41:** 565–573.
24. Lenzen, S. 1978. The immediate insulin secretory response of the rat pancreas to glucose compared with tolbutamide and other secretagogues. *Diabetes.* **27:** 27–34.
25. Klachko, D. M., and T. W. Burns. 1977. Observations on glucose homeostasis using continuous monitoring. *Horm. Metab. Res.* **7**(Suppl.): 64–71.
26. Bagdade, J. D., E. L. Bierman, and D. Porte, Jr. 1967. The significance of basal insulin levels in the evaluation of the insulin response to glucose in diabetic and nondiabetic subjects. *J. Clin. Invest.* **46:** 1549–1557.
27. Field, J. B. 1972. Insulin extraction by the liver. *Handb. Physiol.* **1**(Sect. 7, Endocrinology): 505.
28. Navalesi, R., A. Pilo, and E. Ferrannini. 1976. Insulin kinetics after portal and peripheral injections of ^{125}I-

insulin. II. Experiments in the intact dog. *Am. J. Physiol.* **230:** 1630–1636.
29. Kaden, M., P. Harding, and J. B. Field. 1973. Effect of intraduodenal glucose administration on hepatic extraction of insulin in the anesthetized dog. *J. Clin. Invest.* **52:** 2016–2028.
30. Harding, P. E., G. Bloom, and J. B. Field. 1975. Effect of infusion of insulin into portal vein on hepatic extraction of insulin in anesthetized dogs. *Am. J. Physiol.* **228:** 1580–1588.
31. Röjdmark, S., G. Bloom, M. C. Y. Chou, J. B. Jaspan, and J. B. Field. 1978. Hepatic insulin and glucagon extraction after their augmented secretion in dogs. *Am. J. Physiol.* **235:** E88–E96.
32. Insel, P. A., K. J. Kramer, R. S. Sherwin, J. E. Liljenquist, J. D. Tobin, R. Andres, and M. Berman. 1974. Modeling the insulin glucose system in man. *Fed. Proc.* **33:** 1865–1868.
33. Blackard, W. G., and N. C. Nelson. 1970. Portal and peripheral vein immunoreactive insulin concentration before and after glucose infusion. *Diabetes.* **19:** 302–306.
34. DeFronzo, R. A., R. Andres, T. A. Bledsoe, G. Boden, G. A. Faloona, and J. D. Tobin. 1977. A test of the hypothesis that the rate of fall in glucose concentration triggers counterregulatory hormonal responses in man. *Diabetes.* **26:** 445–452.
35. O'Connor, M. D. L., H. D. Landahl, and G. M. Grodsky. 1977. Role of rate of change of glucose concentration as a signal for insulin release. *Endocrinology.* **101:** 85–88.
36. Chen, M., and D. Porte, Jr. 1976. The effect of rate and dose of glucose infusion on the acute insulin response in man. *J. Clin. Endocrinol. Metab.* **42:** 1168–1175.
37. Albisser, A. M., B. S. Leibel, T. G. Ewart, Z. Davidovac, C. K. Botz, and W. Zingg. 1974. An artificial endocrine pancreas. *Diabetes.* **23:** 389–396.
38. Kerner, W., Ch. Thum, Gy. Tamàs jun., W. Beischer, A. H., Clemens, and E. F. Pfeiffer. 1976. Attempts at perfect normalization of glucose tolerance test of severe diabetics by artificial beta cell. *Horm. Metab. Res.* **8:** 256–261.
39. Kawamori, R., M. Schichiri, Y. Goriya, Y. Yamasaki, Y. Shigeta, and H. Abe. 1978. Importance of insulin secretion based on the rate of change in blood glucose concentration in glucose tolerance assessed by the artificial beta cell. *Acta Endocrinol.* **87:** 339–351.
40. Bergman, R. N., and J. Urquhart. 1971. The pilot gland approach to the study of insulin secretory dynamics. *Recent Prog. Horm. Res.* **44:** 583–605.
41. Grill, V., U. Adamson, and E. Cerasi. 1978. Immediate and time-dependent effects of glucose on insulin release from rat pancreatic tissue. Evidence for different mechanisms of action. *J. Clin. Invest.* **61:** 1034–1043.
42. Guyton, J. R., R. O. Foster, J. S. Soeldner, M. H. Tan, C. B. Kahn, L. Koncz, and R. E. Gleason. 1978. A model of glucose insulin homeostasis in man that incorporates the heterogeneous fast pool theory of pancreatic insulin release. *Diabetes.* **27:** 1027–1042.
43. Reaven, G. M., and J. M. Olefsky. 1974. Relationship between insulin response during the intravenous glucose tolerance test, rate of fractional glucose removal and the degree of insulin resistance in normal adults. *Diabetes.* **23:** 454–459.
44. Bishop, J. S., and J. Larner. 1967. Rapid activation-inactivation of liver uridine diphosphate glucose-glycogen transferase and phosphorilase by insulin and glucagon *in vivo*. *J. Biol. Chem.* **242:** 1354–1362.
45. Gould, M. K., and I. H. Chaudry. 1970. The action of insulin on glucose uptake by isolated rat soleus muscle. II. Dissociation of a priming effect of insulin from its stimulating effect. *Biochim. Biophys. Acta.* **215:** 258–263.
46. Mirouze, J., J. L. Selam, T. C. Pham, and D. Cavadore. 1977. Evaluation of exogenous insulin homeostasis by the artificial pancreas in insulin-dependent diabetes. *Diabetologia.* **13:** 273–278.
47. Mirouze, J., F. Collard, J. L. Selam, and T. C. Pham. 1977. Continuous blood glucose monitoring in insulin-treated diabetics. *Horm. Metab. Res.* **7**(Suppl.): 77–86.
48. Brunzell, J. D., R. P. Robertson, R. L. Lerner, W. R. Hazzard, J. W. Ensinck, E. L. Bierman, and D. Porte, Jr. 1976. Relationship between fasting plasma glucose level and insulin secretion during intravenous glucose tolerance tests. *J. Clin. Endocrinol. Metab.* **42:** 222–229.